

Coherent control of Kerr nonlinearity via double dark resonances (DDRs)

A. Rahelia⁺¹⁾, M. Sahraib*, A. Namdarc[×], R. Sadighi-Bonabid[°]

⁺Aras International Campus, University of Tabriz, 51666 Tabriz, Iran

*Research Institute for Applied Physics, University of Tabriz, 51666 Tabriz, Iran

[×]Faculty of Physics, University of Tabriz, 51666 Tabriz, Iran

[°]Department of Physics, Sharif University of Technology Azadi Ave, Tehran, Iran

Submitted 11 January 2016

Resubmitted 10 February 2016

A theoretical scheme for enhanced Kerr nonlinearity is proposed in a four-level ladder-type atomic system based on double dark resonances (DDRs). We solve the relevant density matrix equations in steady state and utilize the perturbation theory to obtain the analytical expressions for the third order susceptibility of the atomic system. The influence of system parameters on behavior of the first and third order susceptibilities is then discussed. In particular, it is found that an enhanced Kerr nonlinearity with reduced linear and nonlinear absorption is obtained around zero probe detuning under the slow light condition through proper adjusting the laser field intensity and frequency detuning of driving fields. The dressed state analysis is employed to explain the physical origin of the obtained result. The obtained results may be important for all-optical signal processing and quantum information technology.

DOI: 10.7868/S0370274X16060023

1. Introduction. It is known that an external field modifies the linear [1–5] and nonlinear [6–12] optical response of an atomic medium. Electromagnetically induced transparency (EIT) [2], as a phenomenon in which a beam of electromagnetic radiation propagates through a medium with reduced absorption, can be used to generate and even enhance the nonlinear optical processes [12]. Based on atomic coherence which can lead to reduce absorption, EIT has opened up a completely new route to achieving large optical nonlinearity [13]. Kerr-nonlinearity, which is proportional to the refractive part of the third order susceptibility, has widely been investigated in recent years [13–18]. It is desirable to obtain an enhanced Kerr nonlinearity accompanied with reduced probe absorption due to its potential applications in quantum nondemolition measurements [19], quantum teleportation [20], cross-phase modulation [12], and self-phase modulation for generation an optical soliton [21]. A giant Kerr nonlinearity with vanishing linear susceptibility obtained by electromagnetically induced transparency was investigated by Schmidt and Imamoglu [13]. A theoretical investigation of the Kerr nonlinearity via the effect of spontaneously generated coherence (SGC) was carried out by Niu and Gong

[14]. The giant Kerr nonlinearity in a four-level inverted Y-type atomic system is also investigated by Bai et al. [15]. They showed that compared with that generated in a generic three-level system, the Kerr nonlinearity for such atomic scheme can be enhanced by several orders of magnitude with vanishing linear absorption. The third-order susceptibility is also investigated in a five-level atomic system in which the laser beams couple the ground state to a four-level closed-loop system [16]. In a multi-photon resonance condition, the Kerr nonlinearity of such a medium can be enhanced remarkably by the amplitudes and phase control of the applied fields.

It is well known that dark resonance is the basis for coherent population trapping (CPT) [1], EIT [2], adiabatic population transfer [22], and so on. Several works have been done in order to extend the study of EIT from the simple Λ -type three-level system to more complicated schemes including more than three levels. An additional field probing another excitation path can lead to an induced coherence to the system, leading to the phenomenon of double-dark resonances (DDRs). There are fundamentally three different schemes for the presence of DDRs in four-level atomic systems. First, a four-level lambda-configuration system where the final state has two-fold levels [23–26], second, a four-level tripod-configuration system [27–29], and third, a four-

¹⁾e-mail: raheliali.b@gmail.com; raheliali@yahoo.com

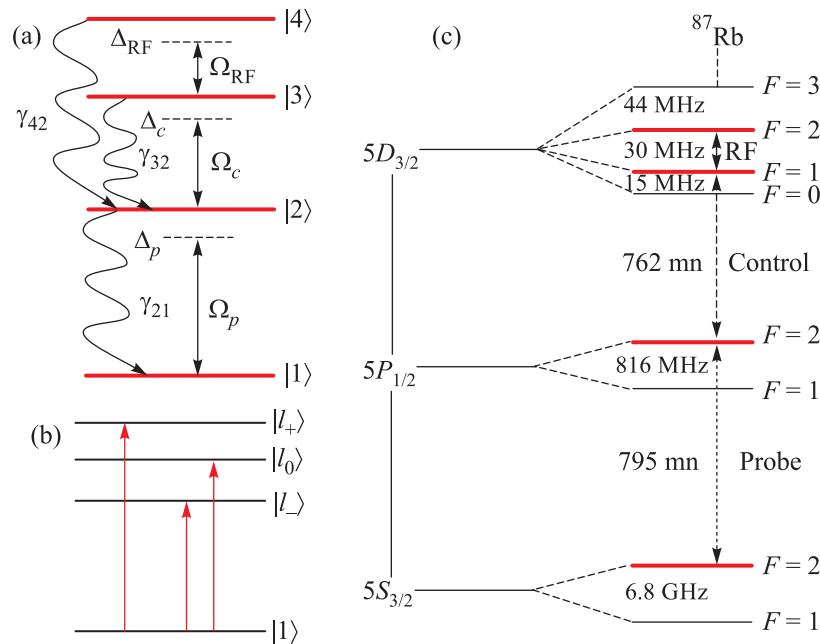


Fig. 1. (Color online) (a) – Schematic diagram of cascade-type four-level atoms with upper two-folded levels interacting with a weak probe laser, a strong cw control laser, and RF driving field. (b) – Dressed state diagram. (c) – Level structure and the laser-coupling scheme for a cascade four-level ^{87}Rb atomic system

level cascade-configuration system where upper state has two-fold levels [30–33]. Note that, coherent control of EIT and electromagnetically induced absorption (EIA) in presence of optical-RF two-photon coupling configurations has been recently studied [24]. Unlike these works, the aim of this proposal is to investigate the possible large Kerr index in pulsed regime for an RF-driven four-level cascade-type atom. Note that the giant Kerr nonlinearity for the four-level lambda-configuration [26] and tripod configuration [29] is already investigated. However, to the best of our knowledge, so far no related individual theoretical or experimental work has been carried out to explore the enhanced Kerr nonlinearity with vanished absorption through such an RF-driven four-level atomic system in cascade-configuration with interacting DDRs, which motivate us for the present study.

Recently, we investigated the behavior of the optical bistability for a medium consisting of a four-level cold atom in ladder-configuration, in which a RF field couples upper two-folded levels [34]. We showed that based on DDRs, one can reduce the threshold of optical bistability and multistability through appropriate modulating the intensity and frequency detuning of the driving fields. We have attributed this reduction on threshold intensity of optical bistability/multistability curves to the effect of Kerr nonlinearity enhancement. Inspired by this study, in this letter we intend to explore theoretically

the behavior of Kerr nonlinearity through a cascade-type atomic medium with upper two-folded levels. Because of interaction with an additional RF field in this four-level cascade-type atomic system driven by a weak probe field and a strong control field, the phenomenon of interfering double-dark states, i.e., DDRs are present. Based on DDRs and as we expected from the previous proposal [34], it is demonstrated that it is indeed possible to obtain large Kerr nonlinearities accompanied with negligible absorption in such a four-level atomic medium by going beyond the steady-state approximation and under the weak probe field approximation. The proposed scheme may provide potential applications in design of logic-gate devices for optical computing and quantum information processing.

2. Model and equations of motion. Fig. 1a shows a four-level atomic system in cascade-configuration coupled by two laser fields and a RF driving field. A weak probe laser with Rabi-frequency (RF) $2\Omega_p$ (amplitude E_p and angular frequency ω_p) is employed to couple $|1\rangle \leftrightarrow |2\rangle$ transition. A strong continuous-wave (cw) control field of Rabi-frequency $2\Omega_c$ with amplitude E_c and angular frequency ω_c is applied to transition $|2\rangle \rightarrow |3\rangle$. An assisting RF driving field with Larmor frequency $2\Omega_{\text{RF}}$ (amplitude E_{RF} and angular frequency ω_{RF}) couples upper two-folded Zeeman sublevels $|3\rangle$ and $|4\rangle$ through an allowed magnetic dipole transition and produce DDRs [30, 34–37]. The correspond-

ing one-half Rabi and Larmor frequencies of the optical fields (Ω_j ($j = p, c, \text{RF}$)) for the relevant driven transitions are defined as $\Omega_p = \mathfrak{P}_{21}E_p/2\hbar$, $\Omega_c = \mathfrak{P}_{32}E_c/2\hbar$, and $\Omega_{\text{RF}} = \mathfrak{P}_{43}E_{\text{RF}}/2\hbar$, where $\mathfrak{P}_{ij} = \vec{\mathfrak{P}}_{ij}\hat{e}_L$ is induced atomic dipole moments (\hat{e}_L is the unit polarization vector of the corresponding laser field).

The corresponding spontaneous decay rates related to the transitions $|2\rangle \leftrightarrow |1\rangle$, $|3\rangle \leftrightarrow |2\rangle$, and $|4\rangle \leftrightarrow |2\rangle$ are γ_{21} , γ_{32} , and γ_{42} , respectively. The transitions $|3\rangle \rightarrow |1\rangle$, $|4\rangle \rightarrow |1\rangle$ are considered to be non-dipole allowed, thus the corresponding decay rates γ_{31} , γ_{41} are set to be zero. The relaxation rate of coherence among states $|3\rangle$ and $|4\rangle$ is negligible and thus can be ignored.

The resulting 4×4 Hamiltonian in the interaction picture and under the rotating-wave approximation can be expressed as ($\hbar = 1$) [30]

$$H_{\text{int}} = \begin{bmatrix} 0 & -\Omega_p^* & 0 & 0 \\ -\Omega_p & \Delta_p & -\Omega_c^* & 0 \\ 0 & -\Omega_c & \Delta_p + \Delta_c & -\Omega_{\text{RF}}^* \\ 0 & 0 & -\Omega_{\text{RF}} & \Delta_p + \Delta_c + \Delta_{\text{RF}} \end{bmatrix}, \quad (1)$$

where related detuning of the probe, control and RF fields with respect to corresponding atomic levels are defined as $\Delta_p = \omega_{21} - \omega_p$, $\Delta_c = \omega_{32} - \omega_c$, $\Delta_{\text{RF}} = \omega_{43} - \omega_{\text{RF}}$.

The dynamical evolution of the atomic system can be evaluated by using the density matrix equations of motion as

$$\begin{aligned} \dot{\rho}_{22} &= -\gamma_{21}\rho_{22} + \gamma_{32}\rho_{33} + \gamma_{42}\rho_{44} + \\ &+ i\Omega_p(\rho_{12} - \rho_{21}) + i\Omega_c(\rho_{32} - \rho_{23}), \\ \dot{\rho}_{33} &= -\gamma_{32}\rho_{33} + i\Omega_c(\rho_{23} - \rho_{32}) + i\Omega_{\text{RF}}(\rho_{43} - \rho_{34}), \\ \dot{\rho}_{44} &= -\gamma_{42}\rho_{44} + i\Omega_{\text{RF}}(\rho_{34} - \rho_{43}), \\ \dot{\rho}_{21} &= -\left(\frac{\gamma_{21}}{2} + i\Delta_p\right)\rho_{21} + i\Omega_p(\rho_{11} - \rho_{22}) + i\Omega_c\rho_{31}, \\ \dot{\rho}_{31} &= -\left[\frac{\gamma_{32}}{2} + i(\Delta_p + \Delta_c)\right]\rho_{31} + \\ &+ i\Omega_c\rho_{21} + i\Omega_{\text{RF}}\rho_{41} - i\Omega_p\rho_{32}, \\ \dot{\rho}_{41} &= -\left[\frac{\gamma_{42}}{2} + i(\Delta_p + \Delta_c + \Delta_{\text{RF}})\right]\rho_{41} + \\ &+ i\Omega_{\text{RF}}\rho_{31} - i\Omega_p\rho_{42}, \\ \dot{\rho}_{32} &= -\left(\frac{\gamma_{21} + \gamma_{32}}{2} + i\Delta_c\right)\rho_{32} + \\ &+ i\Omega_c(\rho_{22} - \rho_{33}) + i\Omega_{\text{RF}}\rho_{42} - i\Omega_p\rho_{31}, \\ \dot{\rho}_{42} &= -\left[\frac{\gamma_{21} + \gamma_{42}}{2} + i(\Delta_c + \Delta_{\text{RF}})\right]\rho_{42} + \\ &+ i\Omega_{\text{RF}}\rho_{32} - i\Omega_p\rho_{41} - i\Omega_c\rho_{43}, \end{aligned}$$

$$\begin{aligned} \dot{\rho}_{43} &= -\left(\frac{\gamma_{32} + \gamma_{42}}{2} + i\Delta_{\text{RF}}\right)\rho_{43} + \\ &+ i\Omega_{\text{RF}}(\rho_{33} - \rho_{44}) - i\Omega_c\rho_{42}, \end{aligned} \quad (2)$$

where $\rho_{11} + \rho_{22} + \rho_{33} + \rho_{44} = 1$. Note that the set of Eq. (2) can be solved to obtain the steady-state linear and nonlinear response of the medium. As known, the linear and nonlinear response of the medium to the applied fields are determined by the first and third order susceptibilities. We will present an analytical solution of the first and third order susceptibilities in the next section.

3. Results and discussion. In the following, the Kerr nonlinearity behavior of the presented medium is numerically investigated. First we derive an analytical solution for the first- and third-order susceptibilities. Then, through some numerical simulations we show that this atomic configuration can be employed as an optical medium to obtain giant Kerr nonlinearities with vanishing probe absorption. We shall consider the probe field to be weak compared to the driving fields. Then, we solve the density matrix equations of the motion given by Eq. (2) in the steady state regime and expand the density matrix elements as

$$\rho_{ij} = \rho_{ij}^{(0)} + \rho_{ij}^{(1)} + \rho_{ij}^{(2)} + \rho_{ij}^{(3)} + \dots \quad (3)$$

The zeroth order solution of $\rho_{11}^{(0)}$ will be identical, i.e., $\rho_{11}^{(0)} = 1$, while the other elements are set to be zero.

Using this condition and substituting Eq. (3) into Eq. (2), the off-diagonal first and third order density matrix elements $\rho_{21}^{(1)}$ and $\rho_{21}^{(3)}$ for the probe field can be obtained as

$$\rho_{21}^{(1)} = i\Omega_p(\Omega_{\text{RF}}^2 - BC)/Z, \quad (4a)$$

$$\begin{aligned} \rho_{21}^{(3)} &= i\Omega_p[(\rho_{11}^{(2)} - \rho_{22}^{(2)})(\Omega_{\text{RF}}^2 - BC) + \\ &+ iC\Omega_c\rho_{32}^{(2)} - \Omega_c\Omega_{\text{RF}}\rho_{42}^{(2)}]/Z, \end{aligned} \quad (4b)$$

with

$$Z = -\Omega_c^2 C - \Omega_{\text{RF}}^2 A - ABC,$$

$$A = \frac{\gamma_{21}}{2} + i\Delta_p,$$

$$B = \frac{\gamma_{32}}{2} + i(\Delta_p + \Delta_c),$$

and

$$C = \frac{\gamma_{42}}{2} + i(\Delta_p + \Delta_c + \Delta_{\text{RF}}).$$

It is well known that the linear and nonlinear response of the medium to the applied fields are determined by linear and nonlinear susceptibility $\chi^{(1)}$ and $\chi^{(3)}$ as

$$\chi^{(1)} = \frac{2N\gamma_{21}^2}{\varepsilon_0\hbar\Omega_p}\rho_{21}^{(1)}, \quad (5a)$$

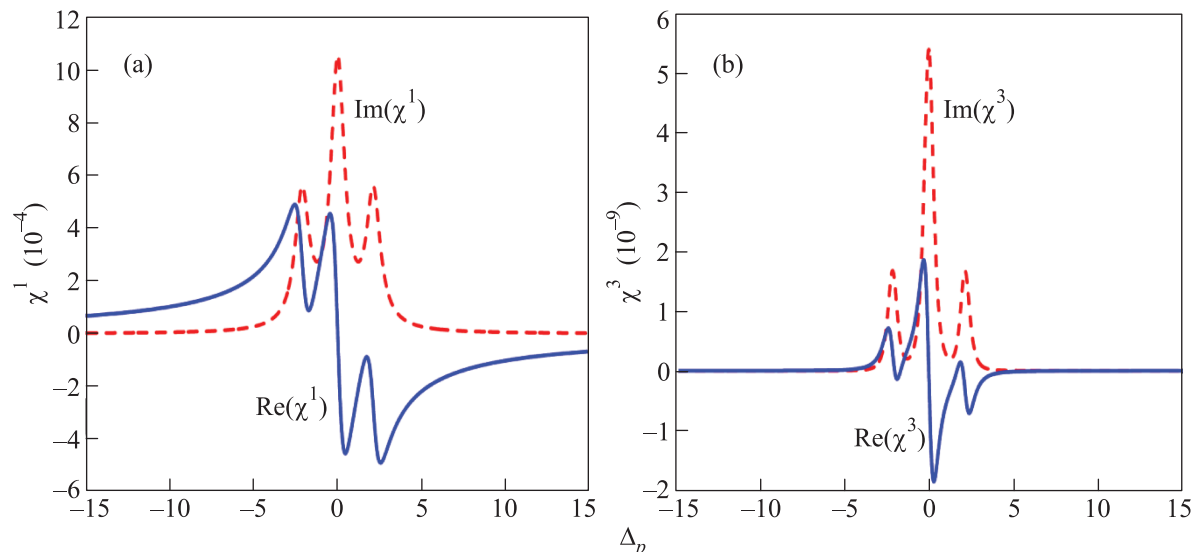


Fig. 2. (Color online) Linear and nonlinear susceptibility versus probe field detuning. (a) – Linear absorption (dashed line) and dispersion (solid line). (b) – Nonlinear absorption (dashed line) and Kerr nonlinearity (solid line). The Selected parameters are $\gamma_{32} = \gamma_{42} = \gamma_{21}$, $\Delta_c = \Delta_{\text{RF}} = 0$, $\Omega_c = 1.5\gamma_{21}$, $\Omega_{\text{RF}} = 1.5\gamma_{21}$

$$\chi^{(3)} = \frac{2N\gamma_{21}^4}{3\epsilon_0\hbar^3\Omega_p^3}\rho_{21}^{(3)}, \quad (5b)$$

where N is the atom density matrix in the medium. The real and imaginary parts of $\chi^{(1)}$ are the linear dispersion and absorption respectively. While the real and imaginary parts of $\chi^{(3)}$ correspond to the nonlinear dispersion (Kerr nonlinearity) and nonlinear absorption. Note that here, $\chi^{(2)}$ does not exist in nonlinear response of the medium because of the symmetry of the atomic system.

Eqs. (4b) and (5b) clearly indicate that the system parameters (i.e., intensity and frequency detuning of coupling fields) affects the third-order nonlinear susceptibility $\chi^{(3)}$, indirectly through atomic coherence between atomic levels. In addition, Eq. (4b) represents that the induced third order optical nonlinearity is related to four terms, which are the second-order coherence terms $\rho_{11}^{(2)}$, $\rho_{22}^{(2)}$, $\rho_{32}^{(2)}$, and $\rho_{42}^{(2)}$.

Based on Ref. [34], we assume $\gamma_{32} = \gamma_{42} = \gamma_{21}$, and all involving parameters are scaled by γ_{21} , which should be in the order of MHz for rubidium atoms. In addition, all the results for the first and third order susceptibilities are plotted in units of $\frac{2N\gamma_{21}^2}{\epsilon_0\hbar\Omega_p}$ and $\frac{2N\gamma_{21}^4}{3\epsilon_0\hbar^3\Omega_p^3}$, respectively. First, we investigate the effect of RF driving field intensity Ω_{RF} on the Kerr nonlinearity behavior for the resonance condition $\Delta_c = \Delta_{\text{RF}} = 0$. Typical linear and nonlinear susceptibilities as a function of probe field detuning are displayed in Fig. 2. We find that for $\Omega_c = \Omega_{\text{RF}} = 1.5\gamma_{21}$, three absorption peaks appear in linear and nonlinear susceptibility profiles and the medium experiences a strong linear absorption. In

this condition, the slope of linear dispersion is negative around $\Delta_p = 0$, which corresponds to superluminal light propagation. The corresponding nonlinear susceptibility is displayed in Fig. 2b. Obviously, a weak Kerr nonlinearity is accompanied with a large linear and nonlinear absorption. Therefore, in this case, the medium is not suitable for application of low-intensity nonlinear optics due to thermal effect of devices. In order to eliminate the thermal effects, we need to propose conditions for Kerr nonlinearity enhancement with reduced absorption in the atomic medium. Fig. 3 shows that how the Rabi-frequency Ω_{RF} affects the linear and nonlinear susceptibilities. It can be seen From Figs. 3a and b that when increasing the Rabi-frequency Ω_{RF} from $1.5\gamma_{21}$ to $3\gamma_{21}$, the peak of two sideband linear and nonlinear absorption reduces, while the central peaks becomes higher. Moreover, the distance between each two adjacent peaks increases by increasing Ω_{RF} . In other words, an increase of Ω_{RF} to the larger values increases the height of central linear and nonlinear absorption peaks whereas two lateral peaks decreases. In addition, the slope of nonlinear dispersion remains yet negative around line center while maintaining large linear and nonlinear absorption. Therefore, one can conclude that increasing Ω_{RF} is even more destructive to obtain large Kerr indices accompanied with negligible linear and nonlinear absorption. Next we explore the effect of decreasing Ω_{RF} on our results. Figs. 3c and d demonstrate that by proper tuning of Ω_{RF} from $1.5\gamma_{21}$ to $0.1\gamma_{21}$, the lateral peaks becomes higher while the central linear and nonlinear absorption peaks disappear at $\Delta_p = 0$. Moreover, the slope of lin-

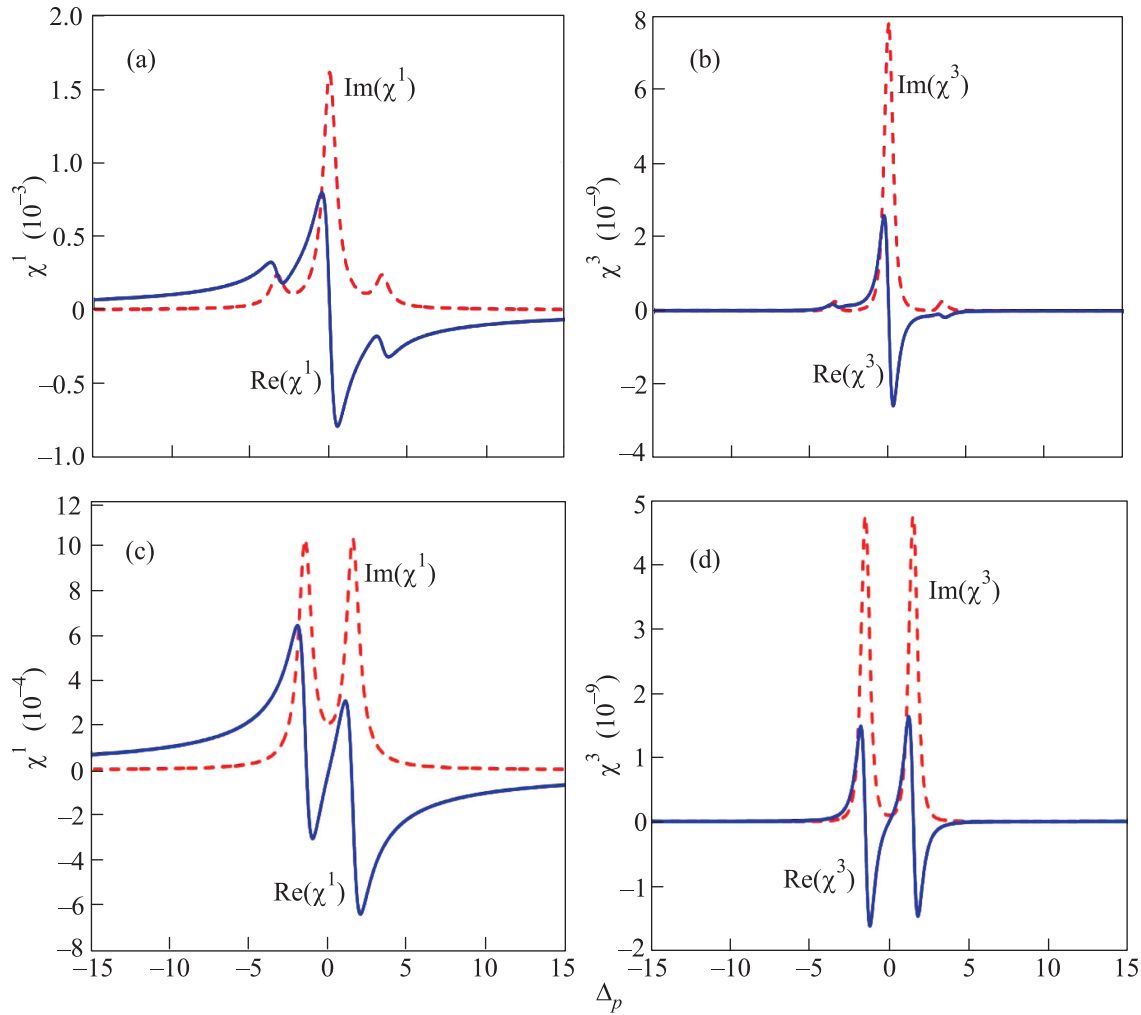


Fig. 3. Color online) Linear and nonlinear susceptibility versus probe field detuning. (a, c) – Linear absorption (dashed line) and dispersion (solid line). (b, d) – Nonlinear absorption (dashed line) and Kerr nonlinearity (solid line). Selected parameters are $\Omega_{\text{RF}} = 3\gamma_{21}$ (a, b) and $0.1\gamma_{21}$ (c, d) Other parameters are the same as Fig. 2

ear dispersion at line center changes from negative to positive that is corresponding to subluminal light propagation. Within this narrow reduced absorption, Kerr nonlinearity is very steep which suggests a giant Kerr nonlinearity with reduced absorption. Thus, simplicity an undesirable case with large absorption can be converted to a convenient case for nonlinear applications just by proper tuning of Rabi-frequency Ω_{RF} .

To understand the physical mechanisms of the above results, we present the dressed state analysis in Fig. 1b. The dressed eigenstates resulted by two control fields Ω_c and Ω_{RF} are, in the general form [38],

$$|l_{\pm}\rangle = \frac{1}{\sqrt{2}}[\Omega_c|2\rangle + \Omega_{\text{RF}}|4\rangle]/\sqrt{\Omega_c^2 + \Omega_{\text{RF}}^2} \mp \frac{1}{\sqrt{2}}|3\rangle, \quad (6a)$$

$$|l_0\rangle = [\Omega_{\text{RF}}|2\rangle - \Omega_c|4\rangle]/\sqrt{\Omega_c^2 + \Omega_{\text{RF}}^2}, \quad (6b)$$

with the corresponding eigenenergies $\varepsilon_{\pm} = \pm\hbar\sqrt{\Omega_c^2 + \Omega_{\text{RF}}^2}$ and $\varepsilon_0 = 0$. For the recondition $\Omega_c = \Omega_{\text{RF}} = \Omega$ as shown in Figs. 2a and b, one can rewrite the dressed states as

$$|l_{\pm}\rangle = \frac{1}{\sqrt{2}} \left[\frac{1}{\sqrt{2}}(|4\rangle + |2\rangle) \mp |3\rangle \right], \quad (7a)$$

$$|l_0\rangle = \frac{1}{\sqrt{2}}[|2\rangle - |4\rangle], \quad (7b)$$

with the eigenenergies being as $\varepsilon_{\pm} = \pm\sqrt{2}\hbar\Omega$ and $\varepsilon_0 = 0$. Eqs. (7) and the corresponding eigenvalues show the origin of the phenomenon of interacting double-dark states resulted in three absorption peaks in linear and nonlinear susceptibility profiles (Figs. 2a and b). In other words, when the frequency detuning of probe field is tuned at $\Delta_p\varepsilon_{\pm}$, and ε_0 , three resonant excitations occur in the dressed-state picture through the pathways:

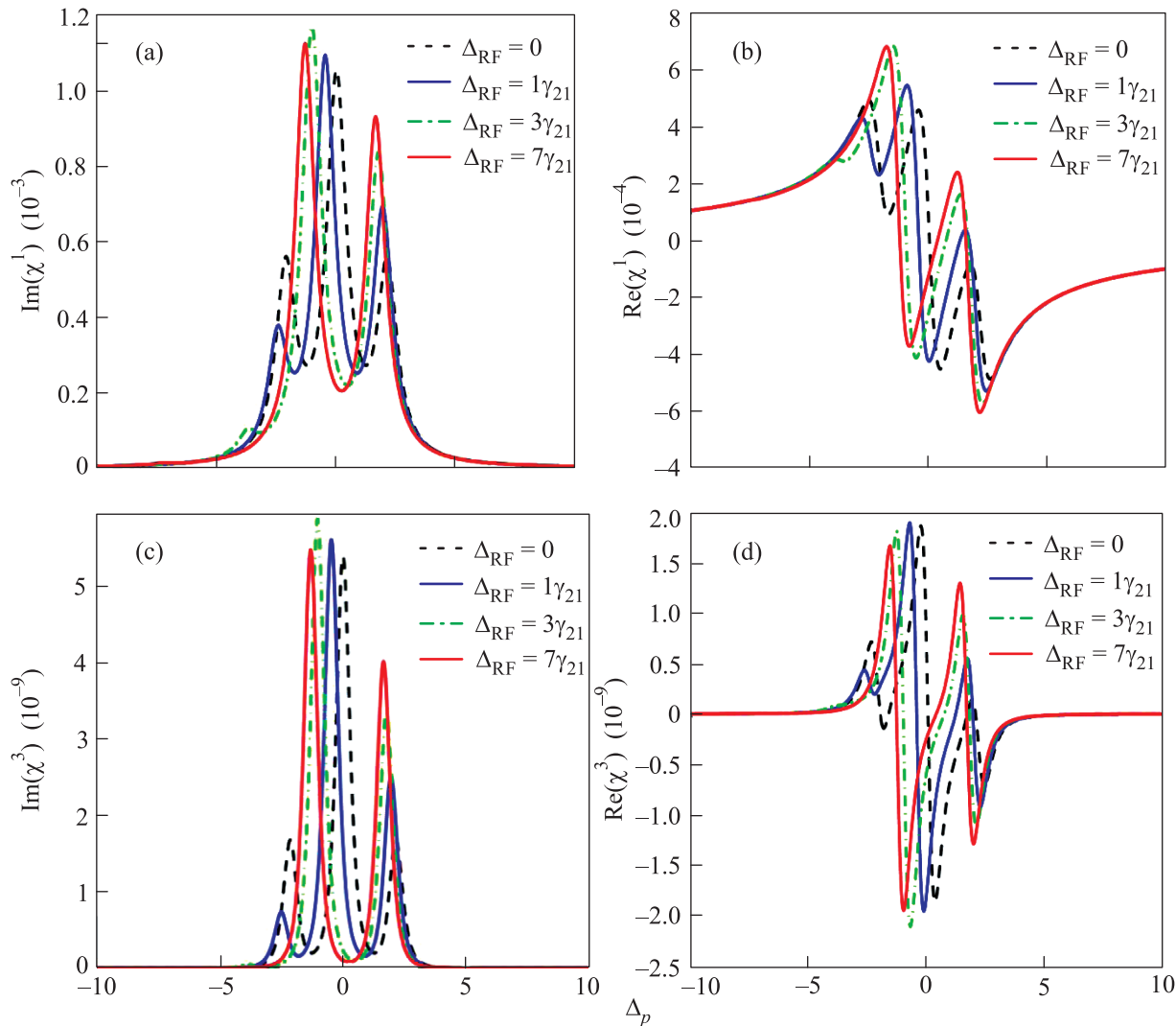


Fig. 4. (Color online) Linear absorption (a), linear dispersion (b), nonlinear absorption (c), nonlinear dispersion (d) versus probe field detuning. Selected parameters are $\Omega_c = \Omega_{RF} = 1.5\gamma_{21}$. Other parameters are the same as Fig. 2

$|1\rangle \xrightarrow{\Omega_p} |l_+\rangle$, $|1\rangle \xrightarrow{\Omega_p} |l_0\rangle$, and $|1\rangle \xrightarrow{\Omega_p} |l_-\rangle$ corresponding to left, central, and right side peaks in Figs. 2a and b. The distance between two lateral peaks is determined by $\varepsilon_+ - \varepsilon_{-\pm} = 2\hbar\sqrt{\Omega_c^2 + \Omega_{RF}^2}$. This explains why the distance between each two adjacent peaks increases by increasing Ω_{RF} which is shown in Figs. 3a and b.

Note that two double reduced absorption regions at both sides of zero probe detuning are induced due to the quantum interference among the three coherent excitation channels as shown in Fig. 1b.

When Ω_{RF} is very weak compared to Ω_c ($\Omega_{RF} \ll \Omega_c$), one can rewrite the eigenstates as

$$|l_{\pm}\rangle = \frac{1}{\sqrt{2}}(|2\rangle \mp |3\rangle), \quad (8a)$$

$$|l_0\rangle = |4\rangle. \quad (8b)$$

Eqs. (8) imply that for very weak Ω_{RF} , the dressed state $|l_0\rangle$ coincides with the bare state $|4\rangle$ and thus will be decoupled from the fields. Accordingly, two peaks separated by splitting energy $2\hbar\Omega_c$ in absorption profile can be obtained because of two dressed states $|l_{\pm}\rangle$ which are attributed to the usual Autler-Townes dressed components (Figs. 2c and d). As a result, the linear and nonlinear probe absorption can be reduced, and the atomic system will be nearly transparent to the probe field at line center $\Delta_p = 0$. This can affect the nonlinear response of the medium, and produce strong nonlinear coupling between the electromagnetic fields interacting with atomic medium resulting in large Kerr nonlinearity at line center (see Figs. 2c and d) [16].

It is known that the linear and nonlinear susceptibility of the medium can be modified with changing

the frequency detuning of driving fields. In order to examine the dependence of nonlinear dispersion to the frequency detuning Δ_{RF} , the curves of linear and nonlinear susceptibility are illustrated in Fig. 4. As can be seen, by increasing Δ_{RF} to the further values, the left-side absorption peaks in linear and nonlinear susceptibility profiles are suppressed, while the central and right-side peaks shift to the left. Thus for the case $\Delta_{\text{RF}} = 7\gamma_{21}$, the linear and nonlinear probe field absorption substantially decreases (Figs. 4a and c). In this case, the slope of linear dispersion converts from negative to positive which represents switching light propagation from superluminal to subluminal (Fig. 3b). Simultaneously, an enhanced Kerr nonlinearity with positive dispersion slope can be achieved for $\Delta_{\text{RF}} = 7\gamma_{21}$ around $\Delta_p = 0$ (Fig. 4d). Thus, we find that increasing the RF driving field detuning leads to enhancement of Kerr nonlinearity accompanied with zero-absorption.

Note that, in order to obtain a large third Kerr nonlinearity, the group velocity must be small because only in this way the optical pulse can interact for a long time in a transparent nonlinear medium [39]. It is known that the slope of dispersion with respect to the probe field detuning plays a major role in the group velocity of probe field. Here we consider the relevant quantity of group index $n_g = c/v$ where c is the speed of light in the vacuum, and the group velocity v_g is given by [40, 41]:

$$v_g = \frac{c}{1 + 2\pi \text{Re}[\chi(\nu_p)] + 2\pi\nu_p \frac{\partial}{\partial\nu_p} \text{Re}[\chi(\nu_p)]}. \quad (9)$$

The group velocity of the probe field strongly depends on the slope of dispersion. It should be pointed that a positive peak in the curves corresponds to subluminal pulse propagation, while a negative dip corresponds to superluminal pulse propagation. The group index behavior of weak probe field is shown in Fig. 5.

It is found from Fig. 5a that for $\Omega_c = \Omega_{\text{RF}} = 1.5\gamma_{21}$, the group velocity corresponds to superluminal light propagation at zero probe detuning. When we increase Ω_{RF} to $3\gamma_{21}$, it can be seen that the condition of superluminal light propagation (negative group velocity) is still existed (Fig. 5b). Setting $\Omega_{\text{RF}} = 0.1\gamma_{21}$, it is clear from Fig. 4c that a subluminal light propagation with positive group velocity is obtained.

Fig. 6 shows the transmission properties of the probe field propagating through the atomic medium. An investigation on Figs. 6a and b show that for both cases $\Omega_c = \Omega_{\text{RF}} = 1.5\gamma_{21}$ and $\Omega_c = 1.5\gamma_{21}$, $\Omega_{\text{RF}} = 3\gamma_{21}$ a low transmission appears at $\Delta_p = 0$, accompanied with two sideband dips (Fig. 6a). By decreasing Ω_{RF} to $0.1\gamma_{21}$, it can be seen from Fig. 6c that the number of transmission dips becomes two. Moreover, a higher transmission

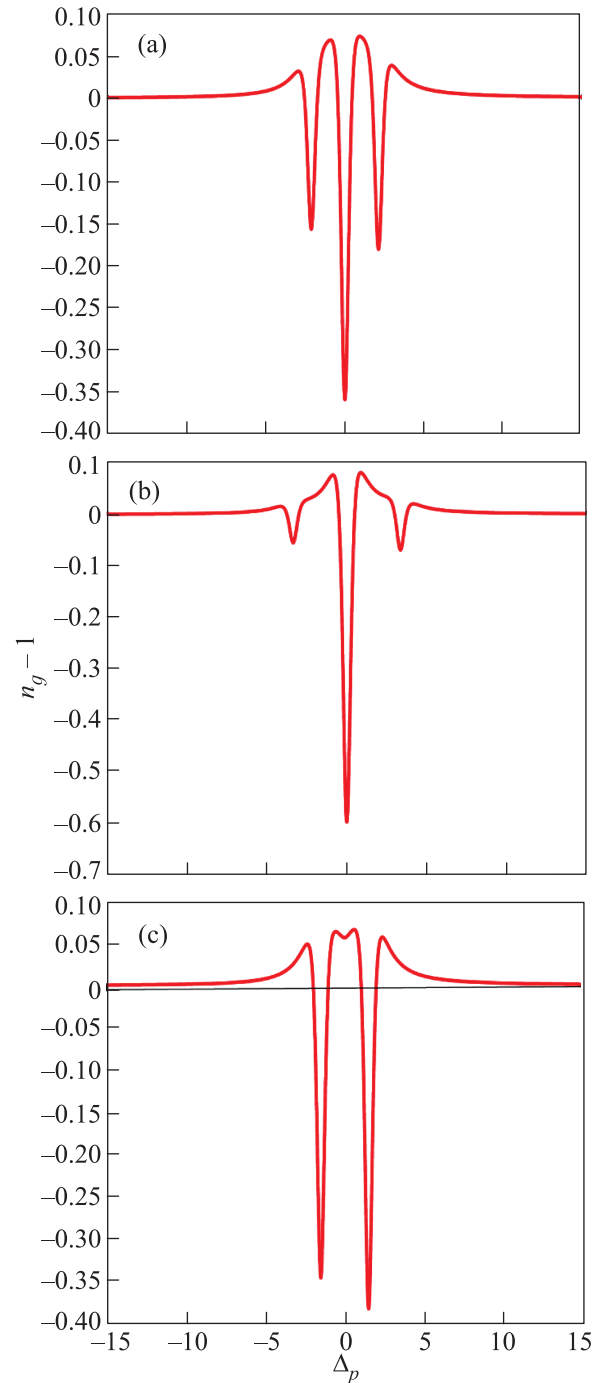


Fig. 5. (Color online) Group index versus probe field detuning. The selected parameters are $\Omega_c = 1.5\gamma_{21}$, $\Omega_{\text{RF}} = 1.5\gamma_{21}$ (a), $3\gamma_{21}$ (b), and $0.1\gamma_{21}$ (c). The other parameters are the same as Fig. 2

coefficient takes place at $\Delta_p = 0$ with respect to Figs. 6a and b.

The impact of the frequency detuning Δ_{RF} on group index as well as transmission coefficient is also plotted in Fig. 7. Obviously, increasing leads Ω_{RF} to a switch from

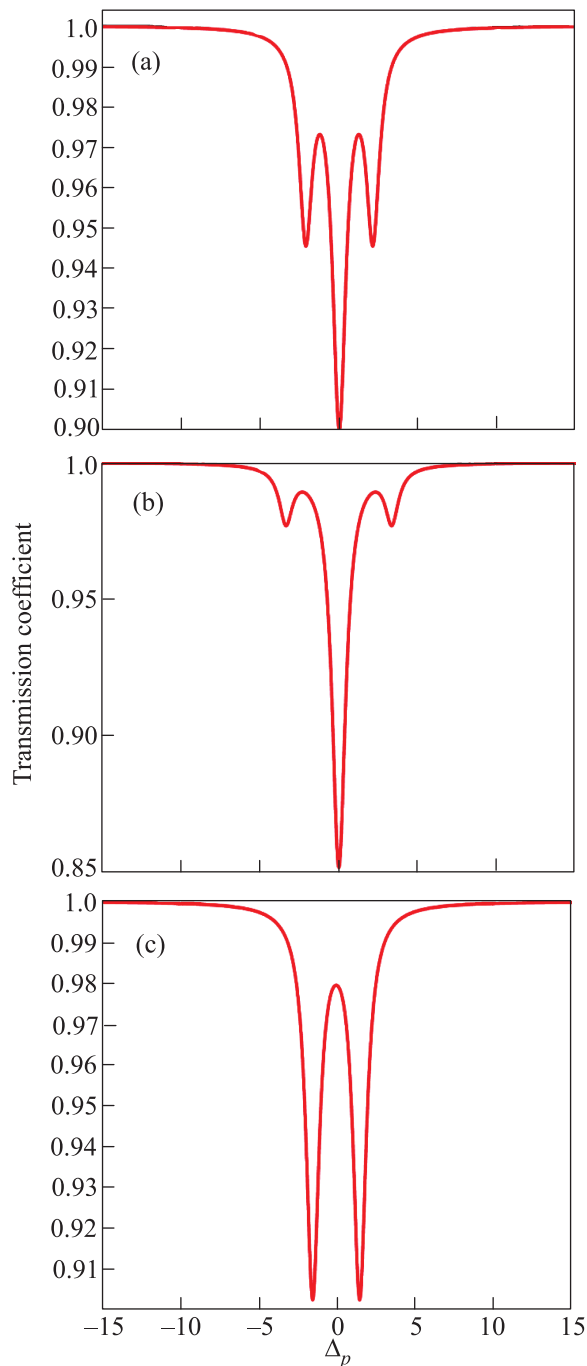


Fig. 6. (Color online) Transmission coefficient versus probe field detuning. The selected parameters are $\Omega_c = 1.5\gamma_{21}$, $\Omega_{RF} = 1.5\gamma_{21}$ (a), $3\gamma_{21}$ (b), and $0.1\gamma_{21}$ (c). The other parameters are the same as Fig. 2

a negative group velocity with superluminal light propagation to a positive group velocity with subluminal propagation of light (Fig. 7a). In addition, a high transmission coefficient takes place instead of a low transmission coefficient at $\Delta_p = 0$ (Fig. 7b).

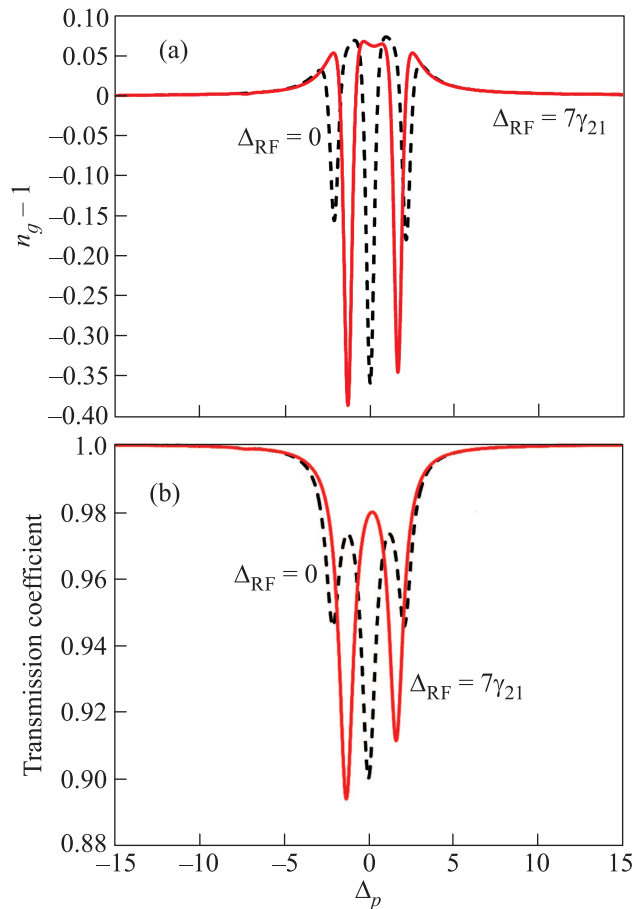


Fig. 7. Group index (a), and transmission coefficient (b) versus probe field detuning. Selected parameters are $\Omega_c = \Omega_{RF} = 1.5\gamma_{21}$. Other parameters are the same as Fig. 2

The obtained results presented in Figs. 5–7 confirm our previous results for nonlinear susceptibility of the probe field in such a four-level atomic medium.

In what follows we explore how the intensity and detuning of the control field Ω_c affects the Kerr coefficient behavior of the medium. We plot in Fig. 8 the representative profiles of real and imaginary part of linear and nonlinear susceptibilities within the probe detuning interval $2\gamma_{21} \leq \Delta_p \leq 3.5\gamma_{21}$. This figure exhibits that when increasing the intensity of Ω_c to $4\gamma_{21}$, a weak Kerr nonlinearity with large linear and nonlinear absorption can be converted to an enhanced Kerr nonlinearity accompanied with negligible absorption and within the condition of slow light propagation.

The influence of control field detuning Δ_c on Kerr nonlinearity behavior is also investigated in Fig. 9. The figures are displayed in the probe field detuning interval $-2.5\gamma_{21} \leq \Delta_p \leq -1.5\gamma_{21}$. As it can be clearly observed, in this detuning interval, the results are similar to that of illustrated in Fig. 5. In other words as shown in Figs. 9a and b, when the control field

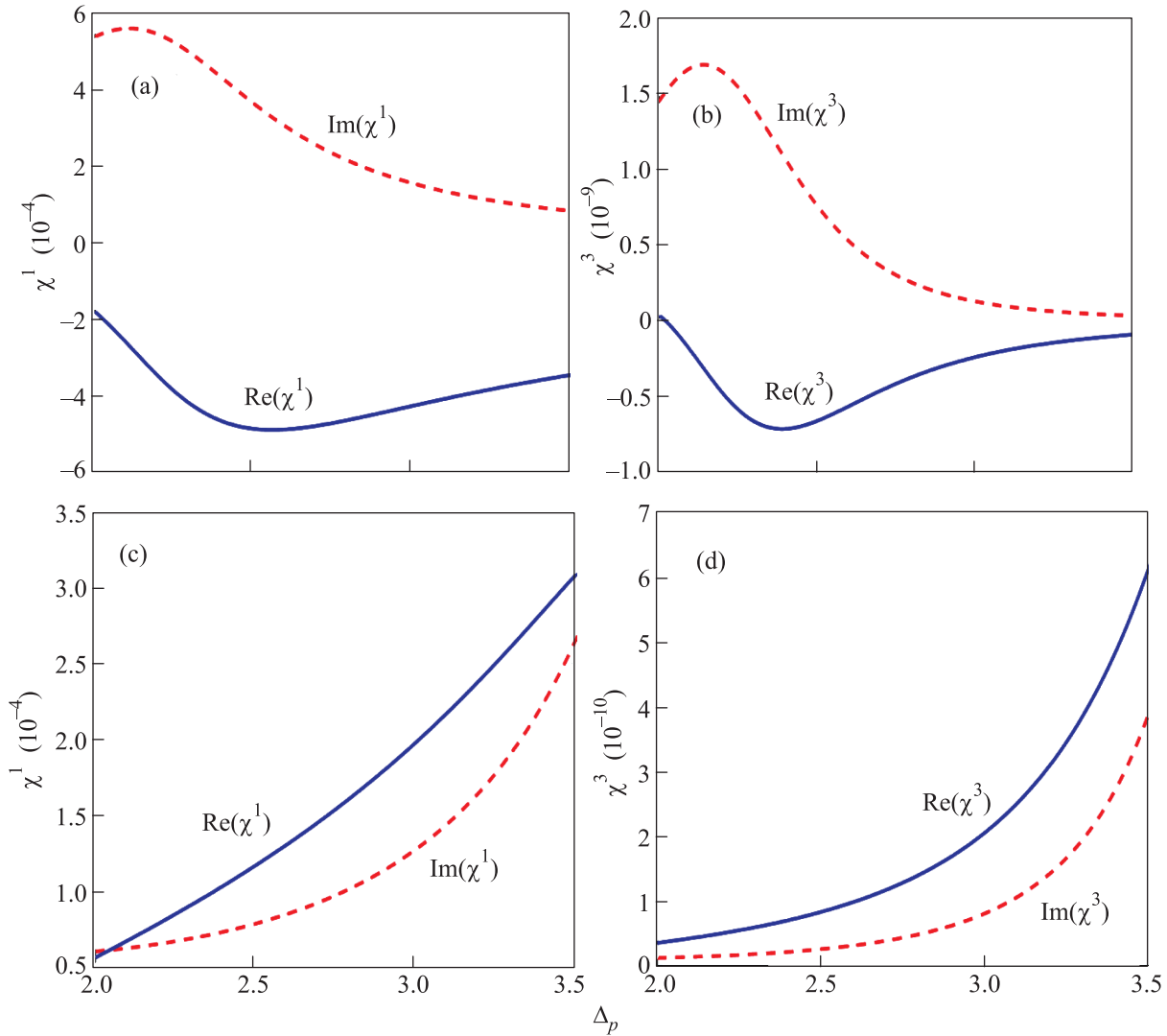


Fig. 8. (Color online) Linear and nonlinear susceptibility versus probe field detuning. (a) – Linear absorption (dashed line) and dispersion (solid line). (b) – Nonlinear absorption (dashed line) and Kerr nonlinearity (solid line). Selected parameters are $\Omega_{\text{RF}} = 1.5\gamma_{21}$, $\Omega_c = 1.5\gamma_{21}$ (a, b) and $4\gamma_{21}$ (c, d). Other parameters are the same as Fig. 2

is in exact resonance with the corresponding transition $|3\rangle \leftrightarrow |2\rangle$, i.e., $\Delta_c = 0$, a weak Kerr nonlinearity is accompanied by strong linear and nonlinear absorption within probe detuning interval $-2.5\gamma_{21} \leq \Delta_p \leq -1.5\gamma_{21}$. The strong absorption along with the Kerr dispersion can destroy the stable propagation of light, so it is not suitable in nonlinear optical applications. When the control field goes out of resonance (say $\Delta_c = 4\gamma_{21}$), an enhanced Kerr nonlinearity can be achieved along with reduced linear and nonlinear probe absorption within $-2.5\gamma_{21} \leq \Delta_p \leq -1.5\gamma_{21}$. Moreover, the light pulse maintains subluminal propagation condition during the whole probe interval $-2.5\gamma_{21} \leq \Delta_p \leq -1.5\gamma_{21}$ (see Figs. 8c and d). Thus, we could present another approach to convert a weak Kerr coefficient to

an enhanced one while reducing absorption of probe field.

Before ending this paper, let us briefly discuss the possible experimental realization of our proposed scheme by means of alkali-metal atoms, appropriate diode lasers, and RF source. Specifically, we consider, for instance, the cold atoms ^{87}Rb (nuclear spin $I = 3/2$) on the $5S-5P-5D$ transitions as a possible candidate [42]. The detailed coupling diagram is shown in Fig. 1c. The designated states can be chosen as follows: $|1\rangle = |5S_{1/2}, F = 2\rangle$, $|2\rangle = |5P_{1/2}, F = 2\rangle$, $|3\rangle = |5D_{3/2}, F = 1\rangle$, and $|4\rangle = |5D_{3/2}, F = 2\rangle$ ($\gamma_{21} \simeq 5.3$ MHz, $\gamma_{32} \simeq 0.67$ MHz, and $\gamma_{42} \simeq 0.67$ MHz) [43] respectively. In this case, the probe field and the control field, whose wavelengths are, respectively, 795 nm ($|1\rangle =$

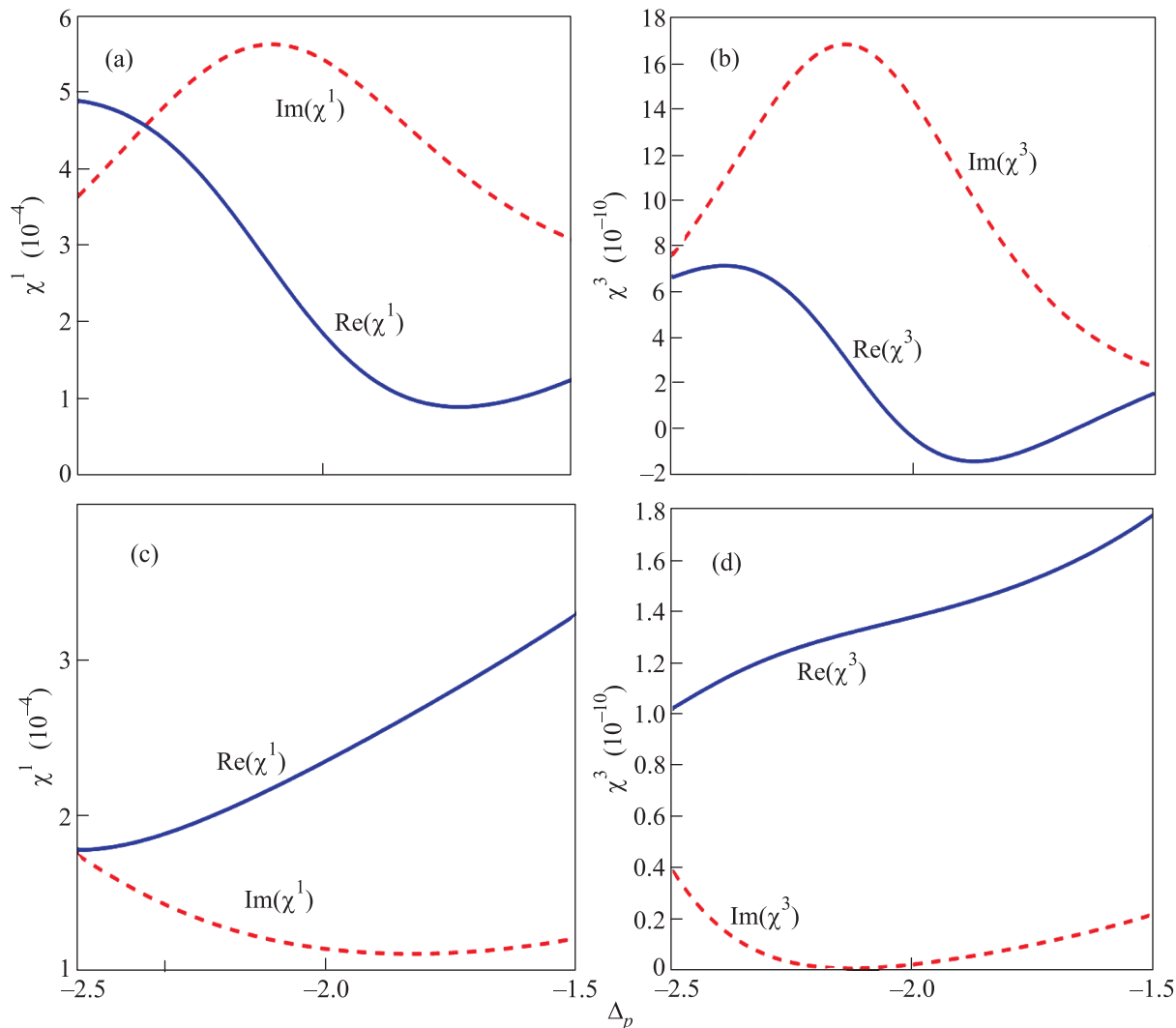


Fig. 9. Linear and nonlinear susceptibility versus probe field detuning. (a) – Linear absorption (dashed line) and dispersion (solid line). (b) – Nonlinear absorption (dashed line) and Kerr nonlinearity (solid line). Selected parameters are $\Delta_{\text{RF}} = 0$, $\Omega_c = \Omega_{\text{RF}} = 1.5\gamma_{21}$, $\Delta_c = 0$ (a, b) and $4\gamma_{21}$ (c, d). Other parameters are the same as Fig. 2

$= |5S_{1/2}, F = 2\rangle \leftrightarrow |2\rangle = |5P_{1/2}, F = 2\rangle$) and 762 nm ($|2\rangle = |5P_{1/2}, F = 2\rangle \leftrightarrow |3\rangle = |5D_{3/2}, F = 1\rangle$) can be obtained from external cavity diode lasers. A 30 MHz RF radiation driving the magnetic dipole transition between $|3\rangle = |5D_{3/2}, F = 1\rangle$ and $|4\rangle = |5D_{3/2}, F = 2\rangle$ comes from a homemade antenna.

5. Conclusion. In this paper, we investigate the Kerr nonlinearity behavior of a four-level ladder-type medium driven by a coherent control field and an assisting radio-frequency (RF) field. We found that an enhanced magnitude of Kerr nonlinearity accompanied by negligible probe absorption can be attained at zero probe detuning just through proper tuning the intensity and detuning of the RF field. Moreover, it is realized that one can manage the magnitude of Kerr nonlinearity in some specific probe frequency detuning intervals

via modulating the intensity and frequency detuning of the control field to achieve large nonlinearities with vanishing linear and nonlinear absorption. The present study may be of interest for researchers in the field of all-optical signal processing and quantum information science.

1. H. R. Gray, R. M. Whitley, and C. R. Stroud, *Opt. Lett.* **3**, 218 (1978).
2. S. E. Harris, *Phys. Today* **50**, 36 (1997).
3. Y. Wu and X. Yang, *Phys. Rev. A* **71**, 053806 (2005).
4. M. Fleischhauer, A. Imamoglu, and J. P. Marangos, *Rev. Mod. Phys.* **77**, 633 (2005).
5. H. R. Hamed, A. Radmehr, and M. Sahrai, *Phys. Rev. A* **90**, 053836 (2014).

6. R. Yu, J. Li, P. Huang, A. Zheng, and X. Yang, *Phys. Lett. A* **373**, 2992 (2009).
7. Y. U. Han, J. Xiao, Y. Liu, Ch. Zhang, H. Wang, M. Xiao, and K. Peng, *Phys. Rev. A* **77**, 023824 (2008).
8. J.-H. Li, *Phys. Rev. B* **75**, 155329 (2007).
9. Zh. Wang and B. Yu, *J. Luminescence* **132**, 2452 (2012).
10. Zh. Wang, A.-X. Chen, Y. Bai, W.-X. Yang, and R.-K. Lee, *J. Opt. Soc. Am. B* **29**, 2891 (2012).
11. Zh.-P. Wang and Sh.-X. Zhang, *Phys. Scr.* **81**, 035401 (2010).
12. Y. Zhang, U. Khadka, B. Anderson, and M. Xiao, *Phys. Rev. Lett.* **102**, 013601 (2009).
13. H. Schmidt and A. Imamoglu, *Opt. Lett.* **21**(23), 1936 (1996); Y. Niu, Sh. Gong, R. Li, Zh. Xu, and X. Liang, *Opt. Lett.* **30**(24), 3371 (2005).
14. Y. Niu and Sh. Gong, *Phys. Rev. A* **73**, 053811 (2006).
15. Y. Bai, W. Yang, and X. Yu, *Opt. Commun.* **283**, 5062 (2010).
16. H. R. Hamed, and G. Juzeliunas, *Phys. Rev. A* **91**, 053823 (2015).
17. D. X. Khoa, L. V. Doai, D. H. Son, and N. H. Bang, *Josa b* **31**, 1330 (2014).
18. X. Yang, K. Ying, Y. Niu, and Sh. Gong, *J. Opt.* **17**, 045505 (2015).
19. Y. F. Xiao, K. Sahin, V. Gaddam, C. Hua, N. Imoto, and L. Yang, *Opt. Express* **16**, 26 (2008).
20. J. Howell and J. Yeazell, *Phys. Rev. A* **62**, 032311 (2000).
21. V. Tikhonenko, J. Christou, and B. Luther-Davies, *Phys. Rev. Lett.* **76**, 2698 (1996).
22. N. V. Vitanov, M. Fleischhauer, B. W. Shore, and K. Bergmann, *Adv. At. Mol. Opt. Phys.* **46**, 55 (2001).
23. G. Fu, X. Li, Z. Zhuang, L. Zhang, L. Yang, X. Li, L. Han, N. B. Manson, and C. Wei, *Phys. Lett. A* **372**, 176 (2008).
24. L. Yang, L. Zhang, X. Li, L. Han, G. Fu, N. B. Manson, D. Suter, and C. Wei, *Phys. Rev. A* **72**, 053801 (2005).
25. C. Y. Ye, A. S. Zibrov, Y. V. Rostovtsev, and M. O. Scully, *Phys. Rev. A* **65**, 043805 (2002).
26. H. R. Hamed, S. H. Asadpour, and M. Sahrai, *Optik* **124**, 366 (2013).
27. E. Paspalakis, N. J. Kylstra, and P. L. Knight, *Phys. Rev. A* **65**, 053808 (2002).
28. A. MacRae, G. Campbell, and A. I. Lvovsky, *Opt. Lett.* **33**, 2659 (2008).
29. X. Yang, Sh. Li, Ch. Zhang, and H. Wang, *J. Opt. Soc. Am. B* **26**(7), 1423 (2009).
30. Y. Wu, J. Saldana, and Y. Zhu, *Phys. Rev. A* **67**, 013811 (2003).
31. D. McGloin, D. G. Fulton, and M. H. Dunn, *Opt. Commun.* **190**, 221 (2001).
32. B. K. Dutta and P. K. Mahapatra, *Phys. Scr.* **75**, 345 (2007).
33. S. N. Sandhya and K. K. Sharma, *Phys. Rev. A* **55**, 2155 (1997).
34. H. R. Hamed, A. Khaledi-Nasab, A. Raheli, and M. Sahrai, *Opt. Commun.* **312**, 117 (2014).
35. S. N. Sandhya and K. K. Sharma, *Phys. Rev. A* **55**, 2155 (1997).
36. D. McGloin, D. G. Fulton, and M. H. Dunn, *Opt. Commun.* **190**, 221 (2001).
37. B. K. Dutta and P. K. Mahapatra, *Phys. Scr.* **75**, 345 (2007).
38. H. R. Hamed and S. H. Asadpour, *J. Appl. Phys.* **117**, 183101 (2015).
39. W. Yan, T. Wang, X. Li, and Ch. Yu, *Philosoph. Mag.* **93**(19), 2514 (2013).
40. L. J. Wang, A. Kuzmich, and A. Dogariu, *Nature* **406**, 277 (2000).
41. C. Liu, Z. Dutton, C. H. Behroozi, and L. V. Hau, *Nature* **409**, 490 (2001).
42. D. Steck, <http://steck.us/alkalidata>
43. M. Yan, E. G. Riskey, and Y. Zhu, *J. Opt. Soc. Am. B* **18**, 1057 (2001).